

Date of publication xxxx 00, 0000, date of current version xxxx 00, 0000.

Digital Object Identifier 10.1109/ACCESS.2023.0322000

A Theoretical Spatial Down-link Interference Model for Low-Altitude Networking

ABSTRACT In the low-altitude networking, signal transmission has no penetration loss, no shadow fading, and less reflection and refraction, with strong coverage. Compared to traditional ground networking scenarios, it faces interference challenges such as a large number of interference cells, a larger range of interference effects, and high interference influence. This article focuses on research on the down-link interference problem which will cause access failure or drop, provides a layered definition of low-altitude stereoscopic networking, summarizes and reveals the coverage and interference characteristics, based on this characteristic and the multiple relationship of multi cell triangular projection, A predicted mathematical model was established for the down-link interference of low-altitude network in the scenario of antenna main-lobe up-tilt. The low-altitude interference prediction model proposed in this paper can predict SINR values and interference cell sets at any position in stereoscopic space, assist in low-altitude route design and optimization, and ensure the performance and service quality of the route network. Simulation experiments have shown that the model can accurately predict, the mean error between the calibrated model's estimated SINR value and the system simulation SINR value is less than 0.2dB, and the standard deviation difference is less than 1.5dB. The accuracy of the main service prediction can reach 100% at the midpoint of the cell.

INDEX TERMS Low-altitude stereoscopic layered networking, Theoretical low-altitude interference model, Theoretical serving cell and interference cell distribution model, 5G cellular networking

I. INTRODUCTION

IN recent years, cellular based networked drones have received widespread attention in the industry. The rapid growth of low-altitude drone express delivery, drone logistics, emergency rescue and other businesses has put forward higher requirements for drone communication links. Compared with other networks such as WiFi, cellular networks support wide area coverage and can achieve beyond line of sight remote flight control of drones [1]. The existing cellular networks are mainly designed to serve ground users, using a coverage method with antennas down-tilt. The propagation environment between ground users and base stations is often dominated by NLOS environment, and the interference from other base stations received by ground users only spreads within a limited range. If existing cellular networks are reused and antenna side-lobes are used to serve low-altitude users [2], the side-lobe coverage is weak and there are issues such as antenna nulling, which cannot meet the low-altitude coverage requirements of over 120 meters [3].

With the rapid development of low-altitude economy, there is also a growing demand for drone based services at altitudes of 300-600 meters. To achieve better coverage performance, the base station antenna can be tilted upwards for coverage. This scenario is mainly based on the LOS (Line of Sight)

path environment [4], where the interference is uncontrolled and forms stereoscopic diffusion propagation. There are more interference cells, stronger interference signal energy, larger interference impact range, and the interference is highly affected. In low-altitude scenarios, up-link interference only exists when there are users conducting business in adjacent low-altitude cells, but even if there are no users residing in low-altitude neighboring areas, down-link interference (such as public channels) still exists, it will cause access failure or drop. This article focuses on down-link interference in low-altitude networking scenarios.

Recently, the research in low-altitude interference mainly focuses on channel model estimation and antenna model design. Reference [5] analyzed the probability of high line of sight (LOS) in low altitude scenarios, which, although helpful for stable transmission and simplified channel model estimation, also brought stronger interference. These interferences can have an impact on the flight performance of drones and threaten flight safety [6]. In reference [7], the impact of coverage on interference under high LOS probability at different antenna inclinations was studied to find the optimal inclination angle. Reference [8] evaluated the interference performance under different channel models. References [9] studied the calculation of the Signal to Interference Plus

Noise Ratio (SINR) for low-altitude antenna down-tilt networking scenarios, while references [10] derived the formula for SIR when antenna up-tilt. However, references [9], and [10] did not mention the impact of hierarchical characteristics at different heights on interference, and did not provide a set of interference neighbors for networking scenarios, making it difficult to accurately predict interference. This article aims to establish a down-link interference model for a low-altitude antenna main-lobe scene, which can more predict the set of interference cells and SINR.

Based on this mode, can optimize other problems of low-altitude networks, such as interference control [11], trajectory optimization [12] [13], energy conservation [14], and positioning [15] [16]. Now, most existing optimizations are based on post-processing methods of intelligent learning [17] [18], lacking pre-processing methods [19] [20]. Due to the attenuation of signals caused by obstacles such as buildings and large trees in traditional ground networking, making it difficult to establish a theoretical model to predict interference for the ground [21]. But in low-altitude thanks to LOS environment, this theoretical model can be established. This article first studies the layered coverage and interference characteristics of low-altitude stereo networking when the base station antenna up-tilt, revealing the characteristics of low-altitude network layering as shown in Fig. 1. A low-altitude interference model based on the multi cell triangular projection multiple relationship is proposed to model the down-link interference of the base station. This model can predict SINR values at any position in the stereoscopic space of low-altitude scenes. This SINR value is related to the hierarchical characteristics of low-altitude stereoscopic networking. The set of interfering cells in different layers is different, and the interfering cell set can be obtained based on the main service and interference cell distribution model proposed in this paper. The system simulation experiment shows that the model can accurately predict low-altitude interference. The mean error between the calibrated model's estimated SINR value and the system simulation SINR value is less than 0.2dB, and the standard deviation difference is less than 1.5dB. The accuracy of the main service prediction can reach 100% at the midpoint of the cell. This model can be well used for predicting and evaluating network interference performance on air routes, and potential interference control and capacity enhancement schemes can be further considered based on this model.

The article mainly consists of the following four chapters: Chapter 1 defines the layering of low-altitude stereoscopic networking and proposes coverage and interference characteristics based on layering; Chapter 2 elaborates in detail on the establishment process of interference prediction model and main service prediction model; Chapter 3 verified the effectiveness of the theoretical model through simulation experiments and calibrated the low-altitude interference model; Chapter 4 summarizes the research findings. The interference mentioned in this article, unless otherwise specified, is con-

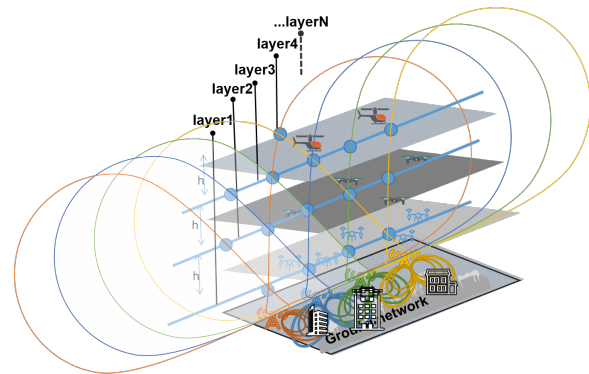


FIGURE 1: Architecture of Low-altitude network layer

sidered down-link interference.

II. DEFINITION AND CHARACTERISTICS OF LOW-ALTITUDE NETWORK LAYERING

Unlike ground networks with antennas down-tilt, when the antenna up-tilt to cover low-altitude, due to the LOS propagation environment, the signal forms stereoscopic diffusion propagation, which not only improves coverage but also brings more complex stereoscopic interference problems. Traditional low-altitude network layering is usually based on business [22]. In order to facilitate the analysis of stereo interference in low-altitude networking, this chapter redefines the layer of low-altitude stereo networking, and proposes the coverage and interference characteristics based on layering. To simplify the analysis, this article assumes that the height of each base station is the same, the spacing between stations is the same [23], the width and tilt angle of the antenna main lobe are the same, and the lower edge of the main lobe beam is aligned with the horizontal plane. In this scenario, the upper edge of the main lobe beam in each cell forms an intersection point, and different layers are formed based on the horizontal lines of each intersection point. Low-altitude stereoscopic network layering has the following coverage and interference characteristics: over the same station, the service cells at different heights are different; At the same height, the service cells on different sites are also different; The service cell and interference cells vary with the change of the layer. Traditional low-altitude networking is often layered based on the provided services. Low-altitude services are currently mainly concentrated in the three-layer area below 600 meters above the ground. The first layer is the ground coverage layer, covering spaces with a height of less than 100 meters, mainly serving unmanned aerial vehicle delivery and other application scenarios; The second layer is an ultra-low altitude coverage layer, covering a space of 100-300 meters above the ground, mainly serving emergency rescue, safety inspections and other application scenarios; The third low altitude coverage layer covers a space of 300-600 meters above the ground, serving application scenarios such as helicopter manned operations. The first layer of coverage is

often obstructed by multiple buildings and vegetation, and the propagation environment is mostly NLOS (Non Line of Sight) [24]; The second and third layers of coverage are aerial coverage with less occlusion, and the propagation environment is mostly LOS (Line of Sight) [25]. This article is mainly based on the analysis of the second and third layers. This paragraph defines the layering of low altitude stereoscopic networking. When the antenna up-tilt, the main lobe of the antenna hits upwards, and the main lobe beams of different cells intersect at different heights in the air. For any two physically adjacent cells, the intersection points formed by the upper edge of the main lobe beam in low-altitude are all on the same horizontal plane. These intersection points are horizontally connected, and the layer formed by this connection is the first layer; Any two small cells physically separated by one cell, whose upper edge of the main lobe beam is at the intersection formed at low-altitude and also on the same horizontal plane, form the second layer after these intersection points are horizontally connected... and so on, any two small cells physically separated by N cells, whose upper edge of the main lobe beam is at the intersection formed at low-altitude and also on the same horizontal plane, form the $N+1$ layer after these intersection points are horizontally connected.

Low-altitude stereoscopic layered network, the height range covered by the main lobe of each cell antenna [26] is limited, and when the inclination angle is small, it cannot cover the top of the station. At this point, there will be a coverage hole above the head of this station, which needs to be covered by the main lobe of the neighboring area. However, the coverage height range of the main lobe of the neighboring area is also limited. At a higher position above the head of this station, it needs to be covered by a farther neighboring area. The low-altitude stereoscopic network layering now does not mention the multi-layer network formed by interweaving beams of each cell at different heights.

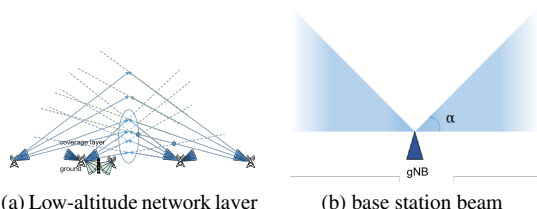


FIGURE 2: Diagram of linear networking

Fig. 2 (a) shows a schematic diagram of low-altitude stereoscopic network layering, where the low-altitude network base station adopts main-lobe coverage, with the beam (blue) directed towards the air, and the beam (green) directed towards the ground of the ground network base station. As shown in Fig. 2 (b), the beam of the low-altitude network base station is divided into two sectors: one to the left and the other to the right, each pointing upwards in their respective directions. The vertical angle of the beam, which defines

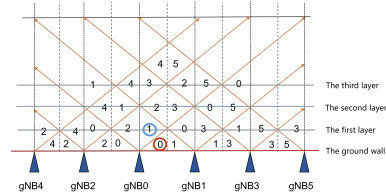


FIGURE 3: Layered of Low-altitude Stereoscopic Network

the range of the beam transmitted by the base station, is α . Assuming that the left and right sectors of the same base station have cell merging. There are also other many enhanced antennas that can be used for reference [27], this article uses 3D antenna [28].

Adjacent areas with different distances from the serving cell on the horizontal plane are called different circles, while adjacent areas with different heights from the serving cell on the vertical plane are called different layers. For example, the first lap adjacent area represents adjacent areas on the same horizontal plane, and the first floor adjacent area represents adjacent areas with different heights on the vertical plane. Fig. 3 shows the hierarchical characteristics of low-altitude stereoscopic networking. The base stations (6 in total) are distributed linearly and equally spaced on the horizontal plane, numbered 0, 1, 2, 3, 4, and 5, with each base station corresponding to a cell. The upper edge of the base station beam is shown by an orange arrow. The red line represents the ground, the blue vertical dashed line represents the vertical bisector of two adjacent base stations, and the black vertical dashed line represents the ground vertical line passing through the base station. If the cell of base station 0 is a serving cell, then base stations 1 and 2 are located in the first circle, and base stations 3 and 4 are located in the second circle..

Due to the layered characteristics of low-altitude scenes, the columnar coverage area above the head of this area has different sets of serving cells and interference neighboring cells. As shown in Fig. 3, users in serving cell 0 (within the red circle) will receive interference from all neighboring cells such as 1, 2, and 3; Users in serving cell 1 (within the blue circle) are only affected by interference from some part of neighboring cells. For example, low-level neighbor 0 with limited coverage height will not interfere with users in the blue circle, while neighboring cells 2 and 3 will interfere. These layered characteristics require the low-altitude interference model to confirm the serving cells and interference cell sets of different layers.

III. LOW ALTITUDE INTERFERENCE PREDICTION MODEL

The low-altitude interference prediction model is based on traditional communication principles and uses mathematical derivation methods such as the Bellman term formula [29] combined with the multi cell triangular projection multiple relationship, to propose an interference model for low-altitude

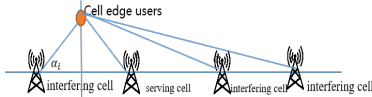


FIGURE 4: Interference in linear networking

stereo networking scenes, under the premise that the user's location satisfies the projection distance of neighboring areas is N times that of the local area. This model can estimate the SINR value of the user's location based on their location, the horizontal projection distance between the service cell and the interfering cell, and the number of interfering cells.

This chapter starts with linear networking scenarios to obtain interference prediction models, and then extends them to cellular networking scenarios through linear interpolation methods, based on the normal direction corresponding to the three sectors of the serving base station. The third section obtains the main service and interfering cells based on the hierarchical characteristics of low-altitude stereoscopic networking.

A. LOW ALTITUDE INTERFERENCE PREDICTION MODEL IN LINEAR NETWORKING SCENARIOS

The low-altitude stereoscopic networking system can use a large angle antenna, taking the 5G system as an example, with a horizontal beam width of 65° and a vertical width of 24° . Ray transmission generates interference when the base station is deployed in a linear two-sector networking scenario. This scenario covers base stations in the same plane and uniform distribution, with each base station using two sector back coverage. Fig. 4 shows the interference between rays, where the red dot represents the position of the user at the edge of the cell and α is between the base station connection line with the user and its ground projection.

The low-altitude interference model in linear networking scenarios is based on the following assumptions:

Assumption 1: The beam is transmitted in a radial manner [30], and interference occurs only when there is an intersection between two beams from different base stations within the same vertical plane in a linear networking scenario.

Assumption 2: The transmission power, antenna gain, and other gains and losses of all base stations are identical and consistent.

Set 'P' as the base station transmission power, 'A' as the base station antenna gain, and 'O' as the sum of other losses. 'O' includes penetration loss, shadow fading, line loss, etc. The path loss (PL) adopts the free space LOS path loss model in 3GPP TS38.901 [31] which is suitable for low-altitude scenario. The formula for PL is $PL=28+22\log_{10}d+20\log_{10}f_c$, where f_c is the center frequency in GHz, d is the distance in meters and PL is measured in dB. In this paper, the center frequency is considered to be 4.9GHz. The interference level

received by users at the ray intersection point is shown in Eq.1:

$$\begin{aligned} I &= P \cdot A \cdot O \cdot \sum_{i=1}^N PL_i = P \cdot A \cdot O \cdot \sum_{i=1}^N B \cdot C \cdot D \\ &= PAOBD \sum_{i=1}^N 10^{-2.2 \log_{10} dis}, \end{aligned} \quad (1)$$

where $B = 10^{-2.8}$, and $D = 10^{-2 \log_{10} f_c}$, and $C = 10^{-2.2 \log_{10} dis}$, and $f_c = 4.9\text{GHz}$, B, C and D are obtained by converting the relevant terms in the path loss formula $PL = 28 + 22 \log_{10} d + 20 \log_{10} f_c$ into linear values. The formula for converting dB values into linear values is given as: $linearValue = 10^{dBValue/10}$.

If $PAOBD = Const$, $dis = d/\cos(\alpha)$ is the straight-line distance from the user to the base station, d is the projection distance from the user to the ground serving cell on the horizontal plane (referred to as the projection distance from the user to the serving cell), and α is the angle between the line connecting the user to the ground serving cell and its projection on the ground.

$$\begin{aligned} I &= Const \sum_{i=1}^N 10^{-2.2 \log_{10} \frac{d_i}{\cos \alpha_i}} \\ &= Const \sum_{i=1}^N 10^{-2.2 \log_{10} \frac{d}{\cos \alpha} \cdot \frac{\cos \alpha}{d} \cdot \frac{d_i}{\cos \alpha_i}}, \end{aligned} \quad (2)$$

where d_i is the projection distance from the user to the i -th interfering cell on the horizontal plane (referred to as the projection distance from the user to the interfering cell), and α_i is the angle between the line connecting the user to the interfering cell and its projection on the ground.

Assumption 3: The beam propagates scattered, at a fixed location, only one beam in a cell generates interference [32].

Assumption 4: $d_i = n_i d$, where the projection distance between the user and the ground interference cell is n_i times that of the ground serving cell.

Assumption 5: $\alpha_i = \arctan(\frac{h}{d_i})$, where h is the height of the user. According to the relationship table between tan angle and numerical value, at that time, $\alpha < 30^\circ$, $\alpha_i \approx \frac{h}{d_i}$ using assumption 4, $d_i = n_i d$, then $\alpha \approx n_i \alpha_i$.

Then Eq.2 can be further represented as Eq.3:

$$I = Const \sum_{i=1}^N 10^{-2.2 \log_{10} \frac{d}{\cos \alpha} \cdot \frac{\cos n_i \alpha_i}{d} \cdot \frac{n_i d}{\cos \alpha_i}} \quad (3)$$

$$\begin{aligned} I &= Const \sum_{i=1}^N 10^{-2.2(\log_{10} \frac{d}{\cos \alpha} + \log_{10} \frac{\cos n_i \alpha_i}{d} \cdot \frac{n_i d}{\cos \alpha_i})} \\ &= Const \cdot 10^{-2.2 \log_{10} \frac{d}{\cos \alpha}} \cdot \sum_{i=1}^N 10^{-2.2 \log_{10} \frac{\cos n_i \alpha_i}{\cos \alpha_i} \cdot n_i}, \end{aligned} \quad (4)$$

where, n_i is the projection distance of the neighboring area n times the projection distance of the service cell.

Using the $\cos nx$ general term formula proposed by mathematician Bellman in 1822, $\cos nx = \frac{(-1)^n \cdot (2n)!}{n!(2n-1)!} \cdot \cos x$ Eq.4, can be expanded to Eq.5.

$$I =$$

$$\text{Const} 10^{-2.2 \log_{10} \frac{d}{\cos \alpha}} \sum_{i=1}^N 10^{-2.2 \log_{10} \frac{(-1)^{n_i} \cdot (2n_i)!}{(n_i-1)!(2n_i-1)!} \cdot n_i}$$

$$\text{SINR} =$$

$$\frac{\text{Const} 10^{-2.2 \log_{10} \frac{d}{\cos \alpha}}}{\text{Const} 10^{-2.2 \log_{10} \frac{d}{\cos \alpha}} \sum_{i=1}^N 10^{-2.2 \log_{10} \frac{(-1)^{n_i} \cdot (2n_i)!}{(n_i-1)!(2n_i-1)!}} + N_0} \quad (5)$$

The denominator is the useful power of the received serving cell, and the numerator is the interference signal power and interference background noise of the received neighboring cells. N_0 is the interference background noise, $N_0 = -174 + 10\log_{10}(BW)$, and BW(Hz) is the bandwidth. The SINR of Eq.5 is a linear value.

Where the background noise is much greater than the interference, SINR calculation is shown in Eq.6:

$$\text{SINR} = \frac{\text{Const} 10^{-2.2 \log_{10} \frac{d}{\cos \alpha}}}{N_0}, \quad (6)$$

,

where the background noise is much smaller than the interference, SINR calculation is as shown in Eq.7.:

$$\text{SINR} = \frac{\text{Const} 10^{-2.2 \log_{10} \frac{d}{\cos \alpha}}}{\text{Const} 10^{-2.2 \log_{10} \frac{d}{\cos \alpha}} \cdot \sum_{i=1}^N 10^{-2.2 \log_{10} \frac{(-1)^{n_i} \cdot (2n_i)!}{(n_i-1)!(2n_i-1)!}}} \quad (7)$$

$$\text{SINR} \approx \text{SIR} \approx \frac{1}{\sum_{i=1}^N 10^{-2.2 \log_{10} \frac{(-1)^{n_i} \cdot (2n_i)!}{(n_i-1)!(2n_i-1)!}}}$$

where N is the number of interference beams or cells, SINR is the signal-to-interference noise ratio, and SIR is the signal-to-interference ratio.

In a linear networking scenario, when the projection distance from the interfering cell to the user is n times of the serving cell to the user, and the vertical angle is $\alpha < 30^\circ$, the interference is related to the relative relationship between the projection distance from the user to the serving cell and the interfering cell, as well as the number of interfering beams or cells. The factors such as user height and beam angle have been considered in the projection distance.

when $n\alpha < \frac{\pi}{2}$ and $\cos n\alpha > 0$. Therefore, the $(-1)^{n_i}$ in Eq.7. can be ignored in the low-altitude interference model in Eq.8:

$$\text{SINR} \approx \text{SIR} \approx \frac{1}{\sum_{i=1}^N 10^{-2.2 \log_{10} \frac{(2n_i)!}{(n_i-1)!(2n_i-1)!}}} \quad (8)$$

In the LOS path scenario of the communication system, there is a high probability that the distance between adjacent cells and users is greater than the distance between serving cells and users [33]. If the relative distance between adjacent cells and serving cells is greater than 1 and \log_{10} (relative distance)

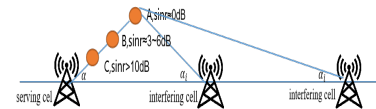


FIGURE 5: Performance of users at different locations

is greater than 0, then the low-altitude interference model can be modified to Eq.9.:

$$\text{SINR} \approx \text{SIR} \approx \frac{1}{\sum_{i=1}^N 10^{|\log_{10} \frac{(2n_i)!}{(n_i-1)!(2n_i-1)!}| - 2.2}} \quad (9)$$

When n_i is relatively small, the Bellman term values of the expansions in Eq.4 and Eq.9 are modified as follows:

1. When $n_i = 1$, $\frac{\cos n_i \alpha_i}{\cos \alpha_i} = 1$;
2. When $n_i = 2$ and $\alpha < 30^\circ$, correct the value of the general term to mean $\frac{\cos n_i \alpha_i}{\cos \alpha_i} = 0.8$.

As analyzed in Eq.9 and Fig.5, if the user is at the edge position of the two stations (as shown in point A in Fig.5), the projection distance of the adjacent area is close to that of the serving cell, and the interference is similar to the useful signal. The SINR value approaches 0, and the user is close to being disconnected. If the user is in the middle of the coverage area of the serving cell (as shown in point B in Fig. Fig.5), the projection distance of the adjacent area is about three times that of the local area, and the interference is about one-third of the useful signal. The SINR value is about 3-6dB, and the user can maintain connection. If the user is located in the center of the serving cell (as shown in point C in Fig.5), the projection distance of the adjacent area is about 6 times that of the local area, and the interference is about 1% of the useful signal. Considering there will be more interference cells, the above estimated performance will suffer.

B. LOW-ALTITUDE INTERFERENCE PREDICTION MODEL IN CELLULAR NETWORKING SCENARIOS

In cellular networks every cell has three-sector. By employing linear interpolation, the two-dimensional linear network's low-altitude interference model can be extended to a three-dimensional interference model. The cellular networking method is shown in Fig.6:

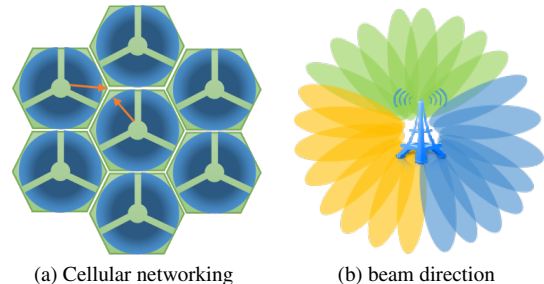


FIGURE 6: Diagram of cellular networking and beam

Expanding the interference model from linear to cellular networking, sampling is conducted in a linear manner. This

ensures that the projected distance from the user's location to all interfering cells is N times the distance to the serving cell. Fig.7 shows two different sampling methods, sampling along the central connecting and sampling along the vertex connection (where the orange dot represents the location of the gNB and the yellow dot represents the location of the users):

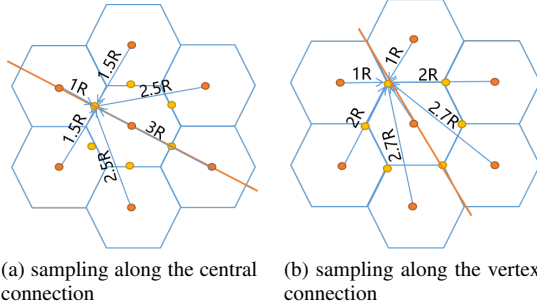


FIGURE 7: Distribution of UEs

(1) Method 1: Sampling along the central connection line of the cell(Fig.7 (a)), and the sampling location is shown in Fig.8 (a):

Sampling along the center-line, the horizontal solid line in the figure represents the connection line to the center of the gNB, the vertical solid line represents the vertical distance from the neighboring base station to the center connection, and the dashed line represents the straight line connection from the neighboring base station to the local base station. y_1 and y_2 are the projection distance from the user to the adjacent area, and x is the projection distance from the user to the local area. The angle β is defined as the angle between the user's connection line in various positions and the center of the gNB, while α is the angle between the user's connection and the cell center. Using α and β , the y/x relationship is determined (where y is the projection distance from the neighboring cell to the user, and x is from the serving cell). In Fig.8 (a), the condition that y/x satisfies the n -fold relationship is derived as follows:

$$\frac{y_1}{x} = \frac{\sin \alpha}{\sin \beta} = \frac{\tan \theta}{\tan \phi} = n, \text{ consequently, } \alpha \approx n\beta \quad (10)$$

where $\theta = \frac{\alpha+\beta}{2}$, $\phi = \frac{\alpha-\beta}{2}$, and consequently $\frac{\tan \theta}{\tan \phi} = \frac{n+1}{n-1}$, when $\theta < 30^\circ$ and $\phi < 30^\circ$, and consequently $\frac{\theta}{\phi} \approx \frac{n+1}{n-1}$, and consequently $\alpha \approx n\beta$. In Eq.10, when α is about n times of β , y_1 is about n times of x . If $\alpha = 60^\circ$, when β is $[10^\circ, 12^\circ, 15^\circ, 20^\circ, 30^\circ]$, y_1 is about n times that of x .

For the second ray y_2 , $\theta > 30^\circ$ and $\phi > 30^\circ$, It is not possible to infer the relationship between y_2 and x in the same way as y_1 . Considering the obtuse triangle, it is assumed that $y_2 \approx x + \sqrt{3}R$, $\sqrt{3}R$ is the distance between stations which is represented by the dashed line, and R is the side length of the cellular cell.

When β is $10^\circ, 20^\circ$, or 30° , $x_1 = 1/3 \cdot \sqrt{3}/2R$, $x_2 = 2/3 \cdot \sqrt{3}/2R$, $x_3 = \sqrt{3}/2R$. The projection distance from the six neighboring cells around the first circle of the serving

cell to the user is n times the projection distance from the serving cell to the user. The relationship between the projection distance of the six adjacent areas in the first circle and the projection distance of the serving cell at three positions is shown in Eq.11, where rows represent users at three positions on the central connecting line, and columns represent the six adjacent areas in the first circle.

$$\begin{Bmatrix} 5, & 6, & 7, & 7, & 7, & 6 \\ 2, & 3, & 4, & 4, & 4, & 5 \\ 1, & 2, & 3, & 3, & 3, & 2 \end{Bmatrix} \quad (11)$$

(2)Method 2: Sampling along the vertex connection line of the cell(Fig.7 (b)), and the sampling location is shown in Fig.8 (b):

y_1 and y_2 are the same as method 1. Adjusts the angle relationship to ensure that y_1 satisfies the n -fold relationship of x , assuming that $y_2 \approx x + \sqrt{3}R$, y_3 can only satisfy the n -fold relationship of x when $1/\sin \beta$ is integer. By querying the Sin table, it can be find that only three angles satisfy this relationship, including $11^\circ, 20^\circ, 30^\circ$.

When β is $11^\circ, 20^\circ, 30^\circ$, $x \approx 1/3R$, $x \approx 2/3R$, $x \approx R$, the relationship between the projection distance of the six adjacent areas in the first circle and the projection distance of the serving cell at three positions is shown in Eq.12. The factorial of 0.5 is expanded using the gamma function, $\Gamma(x+1) = x \cdot \Gamma(x)$, $\Gamma(0.5) = \sqrt{\pi}$ [34].

$$\begin{Bmatrix} 5, & 5, & 7.5, & 7.5, & 5, & 5 \\ 4, & 3, & 4.5, & 4.5, & 3, & 4 \\ 1, & 2, & 2.5, & 2.5, & 2, & 1 \end{Bmatrix} \quad (12)$$

In Fig.8(a), $|AB| = y_1$, $|CB| = y_2$, $|OB| = x$, $\angle BOA = \alpha$, $\angle BAO = \beta$. In Fig.8(b), $|AB| = y_1$, $|CB| = y_2$, $|DB| = y_3$, $|OB| = x$, $\angle BOA = \alpha$, $\angle BDO = \beta$.

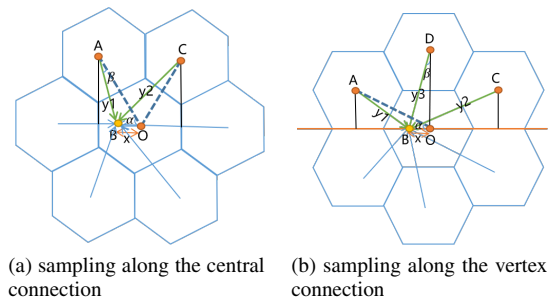


FIGURE 8: sampling location

C. PREDICTION OF LOW-ALTITUDE MAIN SERVICE AND INTERFERENCE CELLS DISTRIBUTION

According to the interference prediction model, the prerequisite for solving the interference amount is to clarify the main service cell and the interfering cells. This section will first study the prediction of the distribution of main service cell and interference cells in linear networking scenarios, and then extend the linear networking scenario to cellular networking.

The interference prediction model for linear networking scenarios is shown in formula 9, in Eq.9,N represents the set of neighboring interfering cells. In low-altitude stereoscopic networking scenarios, the serving cell and interfering cell sets in different layers of vertical high altitude are different. It is necessary to utilize a low-altitude serving and interference cell distribution model to determine the main serving cell where the user is located and the set of adjacent cells which cause interference. The definition of the serving cell in this article adopts the conventional definition, which refers to the cell with the highest power received by the user(UE) from each cell [35].

Unlike the relatively fixed distribution of serving cell on the ground, the distribution of serving cell in low-altitude stereoscopic networking scenarios varies at different heights. The coverage height of antennas with the main-lobe upwards is limited by the downward inclination angle of the antenna. In low-altitude coverage scenarios, there is a problem of black on the tower, that is, there is no coverage over the serving cell, and adjacent areas form cross area [36] coverage over the serving cell. The tower black coverage of the ground cell and the cross area coverage of adjacent areas form a layered coverage of the serving cell. Low level cells have less interference with high level cells at the same horizontal position due to limited coverage height.

The low-altitude stereoscopic networking has brought new interference problems, which are different from traditional overlapping coverage, weak coverage, and over coverage. They all belong to the problem of cell edge coverage, and have added the problem of penetration coverage in the center of the cell. Infiltration coverage refers to the center of this area is covered by other neighboring areas at different heights . According to the low-altitude interference model in Chapter 2, the cells that meet the conditions of Eq.13 are the serving cells:

$$\begin{aligned} PCI - ID &= \max_{i \in [1, N]} Const \cdot 10^{-2.2 \log_{10} dis} \\ &= \max_{i \in [1, N]} Const \cdot 10^{-2.2 \log_{10} \sqrt{h_i^2 + d_i^2}} \end{aligned} \quad (13)$$

where PCI-ID is serving cell physical ID, i is the cell around the UE.

As shown in Fig. 9, with ground serving cell0 as the center and 1/2 of the station spacing as the radius, in the cylinder above ground serving cell0, the low-altitude serving cell is layered , and the PCI (physical cell ID) set of adjacent areas corresponding to the triangular space on the left is the list of adjacent areas on the on the right side of the ground serving cell 0; The PCI set of adjacent areas corresponding to the triangular space on the right is the list of adjacent areas on the left side of the ground serving cell 0.

The three-point positioning method is proposed to calculate the main service cell and its neighboring cell list set of users at any point in space. As shown in Fig. 10, based on the normal direction of the serving cell and connected along the center of the cell, a cell that is in the same direction as the normal direction of the local area is called the right side cell

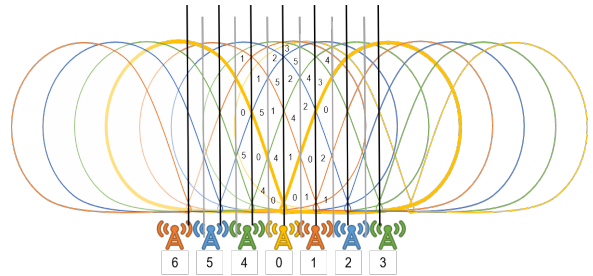


FIGURE 9: Diagram of Low-altitude serving cell

of the local area, while a cell that is in the opposite direction is called the left side cell . The new definitions of left and right boundary lines, left and right triangles, and left and right adjacent areas are as follows:

Definition 1: The right boundary is the vertical direction between the central connecting lines of two stations, which is the right boundary and is layered according to $[(2n-1) h]$; The left boundary is based on the vertical direction of the base station position in the serving cell, and is layered according to $[(2n) h]$.

Definition 2: Right triangle, with vertices on the right boundary; Left triangle, with vertices on the left boundary.

Definition 3: List of right adjacent areas, from ground to high altitude, and the PCI list corresponding to the right triangle is the list on the right side of the adjacent area of the ground center connecting line in this area in sequence; The list of adjacent areas on the left, corresponding to the PCI sequence in the direction of the left triangle towards the sky, is the list on the left of the adjacent area of the ground center connecting line in this area.

The three-point positioning method is as follows:

- 1) Determine the stratification points of the left and right boundaries in this area. The starting point of the vertical direction of the left boundary layer is marked as 0 in this area, with an interval of $h = 2 \cdot x \tan \alpha$. The starting point of the right boundary layer is $x \tan \alpha$, with an interval of $h = 2 \cdot x \tan \alpha$. Where α is the downward inclination angle of the base station antenna, and x is 1/2 of the station spacing.
- 2) The user position is $[x_0, y_0]$,and two parallel lines (with a slope of $\tan \alpha, -\tan \alpha$), intersect with the left and right boundary lines, and the intersection point of the left boundary line is $[y_0 - x_0 \cdot \tan \alpha, y_0 + x_0 \cdot \tan \alpha]$, the intersection point of the right boundary is $[y_0 + x_0 \cdot \tan \alpha - h, y_0 - x_0 \cdot \tan \alpha + h]$.
- 3) If $(y_0 - x_0 \cdot \tan \alpha)/h = (y_0 + x_0 \cdot \tan \alpha)/h = M$ ('/represents fetch), where M is the number of layers, then the serving cell $PCI = rightlist \{L | L \in N, L = M\}$, indicating that the serving cell PCI belonging to the user's location is equal to the M-th cell in the right adjacent cell list. If $(y_0 - x_0 \cdot \tan \alpha)/h \neq (y_0 + x_0 \cdot \tan \alpha - 2h)/h$, then the serving cell $PCI = leftlist \{L | L \in N, L = (y_0 + x_0 \cdot \tan \alpha - h)/h = M\}$, indicating that the serving cell PCI where the user is

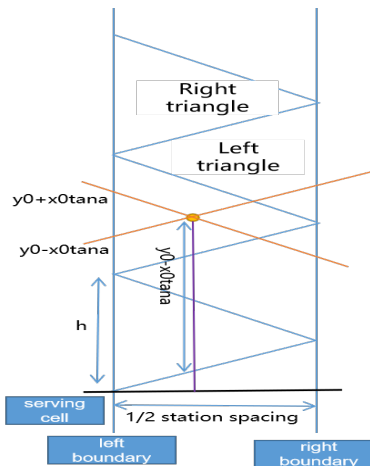


FIGURE 10: Low-altitude serving cell model

located belongs to the M-th in the left neighbor list.

The low-altitude interference prediction model first determines the user's ground service cell based on the user's horizontal projection position, and then confirms the main service cell and neighboring cell list set corresponding to the user's location based on the user's height and the low altitude main service and interference cell distribution model. Consider the main service and interference with the cell, the low-altitude interference prediction model has been updated to Eq.14:

$$SINR \approx \frac{1}{\sum_{i=1}^N 10^{\lfloor \log_{10} \frac{(2n_i)!}{(n_i-1)!(2n_i-1)!} \rfloor - 2.2} + N_0} \quad (14)$$

In Eq.14, $N = \text{rightlist } \{L | L \in N, L > M\} \cup \text{leftlist } \{L | L \in N, L > M\}$, the neighbor list set represents the interference suffered by the user is the neighbor list set above the M-th layer in the left and right neighbor lists.

Based on formula 14, the main service and interference cell distribution in linear networking scenarios can be obtained. This distribution can be extended to cellular networking scenarios, where typical cellular networking uses a 3-sector networking approach. Considering that users are mainly affected by interference in the main lobe direction of neighboring cells, the interference neighboring cells in cellular networks are basically the same as those in linear networks. By linearly extending the normal direction of each sector of the main service base station outward, a list of neighboring cells on the left and right ends can be obtained. Then, according to the model under linear networking, a low-altitude main service and interference cell distribution prediction model under cellular networking can be obtained.

IV. SIMULATION AND VERIFICATION OF THE MODEL

This chapter first built a low-altitude stereoscopic network simulation platform, selected 48 different user locations, and conducted system simulation. The simulation obtained SINR values and service cell identification for each user location,

TABLE 1: System simulation parameter

Simulation parameters	Value
frequency	4.9GHz
Bandwidth	100MHz
stationspacing	2000m
Basestationheight	100m
UEheight	0m, 200m, 400m, 600m
Antennatiltangle	20°
Antennatype	TR368733DAntenna
Channelfadingtype	claussen3DUMa
Transmittingpower	200W
Numberofterminaltransmittingantennas	2
Numberofterminalreceptionantennas	4

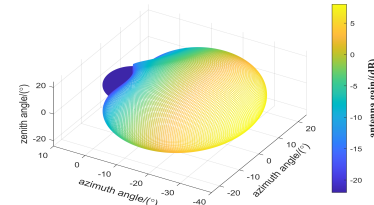


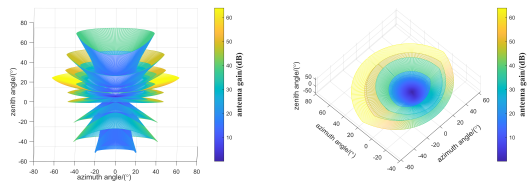
FIGURE 11: Antenna pattern when the downward inclination angle of the antenna is 0 degrees

and compared them with values calculated based on theoretical models. Finally, based on the simulation results, the theoretical model was calibrated to improve its prediction accuracy.

A. EXPERIMENTAL SETUP

The simulation platform utilizes the Vienna University's open platform "LTE System Simulation Platform" to validate the low-altitude interference model. A MIMO (multi-input multi-output) channel module was added on the original platform, and the platform parameters were modified are shown in Tab.1.

In simulating low-altitude scenarios, the channel utilizes Line-of-Sight (LOS) path transmission, excluding shadow fading, penetration loss, and fast fading. The antenna model is shown in Fig. 11 to Fig.13.



(a) Vertical antenna pattern (b) Horizontal antenna pattern

FIGURE 12: The original antenna tilts up by 20 degrees

During the product implementation process, side-lobes can be suppressed to increase the main-lobe coverage performance and reduce the impact of side-lobe coverage. The antenna after suppressing side-lobes is shown in Fig. 13.

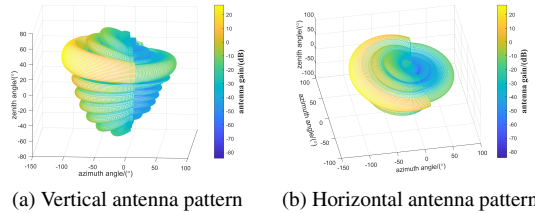


FIGURE 13: The Side-lobe suppression antenna tilts up by 20 degrees

B. SIMULATION RESULT

(1) Low-altitude interference prediction

According to the positional symmetry relationship, 48 points are selected within the region to reflect the overall region, as shown in Fig. 14. Among them, points 13-16/19-32/45-48 are located at 1/3, 2/3, and 3/3 of the cell center line and cell vertex line. The interference model is used for calculation, and other points are interpolated based on these 12 points to obtain predicted values. Based on the user's horizontal and vertical positions, obtain model predicted values and system simulation values, and compare the two values at different heights as shown in Fig.15. Note that the SINR in the Fig.15 has been converted from the linear value of Eq.14 to the dB value.

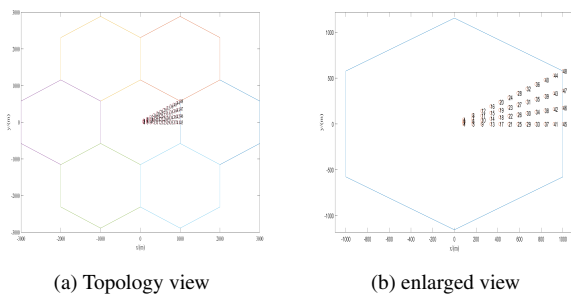


FIGURE 14: UE positions

Based on the preliminary comparison results, it can be concluded that the predicted values of the model are consistent with the trend of the system simulation values, but there are differences in specific values that model calibration is required. In the model, it is assumed $\alpha_i \approx \frac{h}{d_i}$, there is a difference between the predicted data of the model and the platform simulation data due to the use of the Bellman expansion term and channel mode [37]. Based on the existing model prediction, an adjustable function $f(h)$ is added to correct where h denotes the user height. For example, setting the ratio between the average simulation result and the predicted value of the theoretical model as an adjustable constant, and adjusting the theoretical expected value at different heights, as shown in Eq.15.

$$E = \frac{\text{average}(SINR_{simu})}{\text{average}(SINR_{predict})} \quad (15)$$

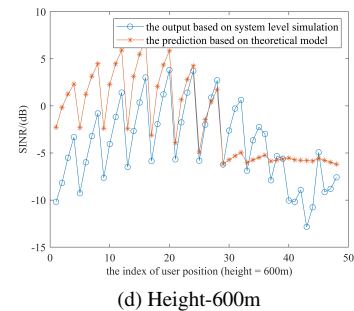
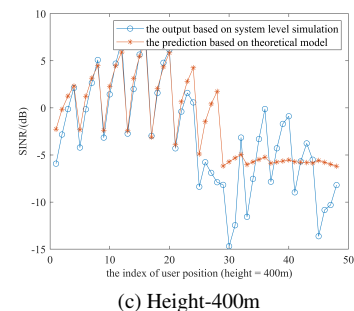
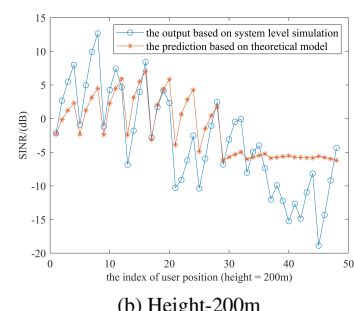
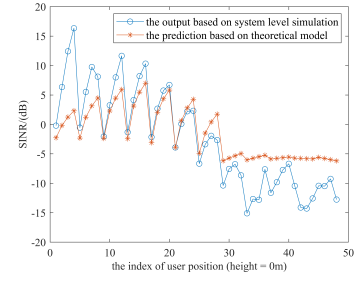


FIGURE 15: Comparison of theoretical interference model prediction and system simulation at the same position

TABLE 2: Differences between model prediction and system simulation before and after adjustment

Height	Standard deviation and mean error of difference before adjustment	Standard deviation and mean error of difference after adjustment	Adjustment value E
0m	3.1/-1.5	1.2/-0.16	2.67
200m	1.5/0.24	1.4/0.19	1.04
400m	0.5/-0.1	0.6/0.05	0.88
600m	0.8/-0.6	0.8/-0.32	0.71

The difference between the model prediction and system simulation before and after adjustment is shown in Tab.2. After adjustment, the difference between the model prediction value and the system simulation value is smaller.

According to the adjusted value E, it was found that there is an exponential relationship between the difference and height. Using linear fitting to obtain the adjustment function, $f(h) = E \cdot (\frac{h}{200} + 1)$, $E \approx 2.5$, is the default value used in the text related to the environment, where h is the user's height in meters.

(2) Low-altitude main service and prediction of interference community distribution

Comparing the theoretical model of low-altitude serving cell distribution with system simulation data, as shown in Fig 16, the PCI of serving cells at different heights is basically the same, and the prediction accuracy of main service is as high as 70%. The prediction rate of the midpoint position in the cell is 100%, while there are differences in the edge areas due to system simulation platform interference and randomization, which reduces the prediction accuracy. In the future, algorithm enhancement will be considered to further improve calibration accuracy.

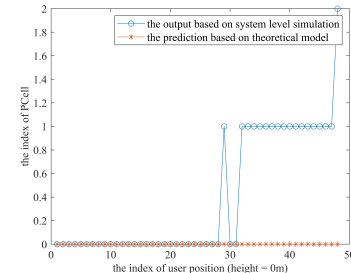
C. MODEL CALIBRATION

The interference model of users at different positions in low-altitude stereoscopic networking scenarios is shown in Eq.16 (When the noise is much smaller than the interference).

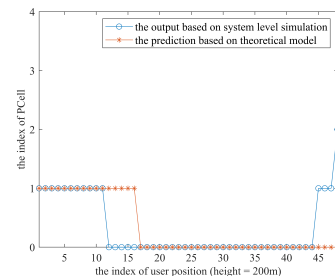
$$SINR \approx \frac{\rho \cdot (\frac{h}{200} + 1)^{-1}}{\sum_{i=1}^N 10^{|\log_{10} \frac{(2n_i)!}{(n_i-1)!(2n_i-1)!}| - 2.2}} \quad (16)$$

. Wherein, $N = rightlist \{L|L \in N, L > M\} \cup leftlist \{L|L \in N, L > M\}$.

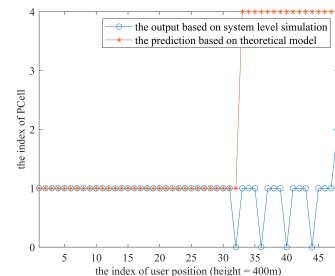
In the Eq.16, N is the number of interfering cells, n_i is a multiple of the projection distance from the interfering cell to the user, to the distance from the serving cell to the user. Rightlist and leftlist are lists of left and right neighboring cells, indicating that the interfering neighboring cell set of the user is the upper left and right neighboring cells of the M layer of the serving cell, and the interference of the lower neighboring cells is relatively small, ρ is a constant, this paper sets the average value of the difference between the theoretical model and simulation results to a constant of 2.5, which is related to the environment.



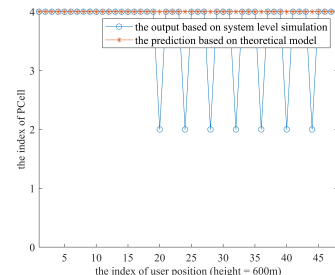
(a) Height-0m



(b) Height-200m



(c) Height-400m



(d) Height-600m

FIGURE 16: Comparison of serving cell model prediction and system simulation at the same location

This interference model, under the condition of a well-defined network plan, can estimate interference, SINR, and serving and interference cell PCI of the user's location can be estimated based on the user's horizontal position and height, guiding and optimizing the operation of low-altitude networking. According to the interference model analysis (Eq.16), in low-altitude stereoscopic networking scenarios, the more adjacent areas, the greater the interference; The smaller the distance between stations, the more layered the space. By reducing adjacent areas, interference can be reduced; By increasing station spacing, can reduce handover times, this pattern can guide the construction of low-altitude networking to improve network performance. However, a decrease in the number of neighboring cells and an increase in station spacing will reduce the capacity of the cell, which is more suitable in scenarios where low-altitude capacity demand is not significant.

V. CONCLUSION

The use of base station antenna up-tilt and antenna main lobe coverage in low-altitude can better meet the low-altitude coverage requirements at higher altitudes, but it faces complex interference problems due to LOS (Line of Sight) propagation. The interference patterns and theoretical prediction models in this scenario are still blank in the industry. This article first analyzes the low-altitude stereo networking based on layered coverage and interference characteristics when the antenna tilts upwards, with different sets of service cells and interference cells in different layers; Proposed a main service and interference cell distribution model, which can obtain a set of interference cells at any location; A mathematical model for down-link interference in low-altitude networks is proposed based on the set of interfering cells and the relationship between multiple cell triangular projection multiples. The SINR value can be obtained at any position in the three-dimensional space with tilted antennas. In Line-of-Sight (LOS) environments, the mean square error difference between the revised model and simulations is less than 0.2dB, and standard deviation difference less than 1.5dB. This model has prediction bias in scenarios with poor channel environment (cell edge), and further enhancement is needed. In addition, Non-Line-of-Sight (NLOS) environments and scenarios with high barriers, the ray propagation pattern deviates from linearity, and factors like reflection and refraction become more prominent. In such cases, further refinement of this model is necessary.

The typical interference, SINR, and PCI distribution in low-altitude stereoscopic networking scenarios can offer technical support for subsequent low-altitude network deployment and business development. For instance, by predicting interference levels and serving cell conditions based on user locations in advance, optimization recommendations can be proposed for route design. This ensures that users experience improved network performance and business support while traveling along those routes. In the future, potential interference control

and capacity enhancement strategies can be explored based on this low-altitude interference model.

ACKNOWLEDGMENT

First of all, I would like to give my heartfelt thanks to all the people who have ever helped me in this paper.

My sincere and hearty thanks and appreciations go firstly to my company, for providing me with positive research areas and soil. Secondly, I must express my sincere thanks to my guider, Cao.lei, Li.xin, JiangTianming, for giving me a lot of very good recommendation.

I am also extremely grateful to all my colleagues and my family who have kindly provided me assistance and companionship in the course of preparing this paper. Finally, I am really grateful to all those who devote much time to reading this thesis and give me much advice, which will benefit me in my later study.

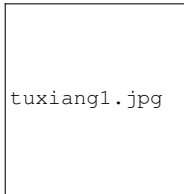
REFERENCES

- [1] Y. Zeng, Q. Wu, and R. Zhang, "Accessing from the sky: A tutorial on uav communications for 5g and beyond," *Proceedings of the IEEE*, vol. 107, no. 12, pp. 2327–2375, 2019.
- [2] Qualcomm, "Paving the path to 5g: optimizing commercial lte networks for drone communication," <https://www.qualcomm.com/news/onq/2016/09/paving-path-5g-optimizing-commercial-lte-networks-drone-communication>, (2016-09-06).
- [3] G. T. 36.777, "Technical specification group radio access network: study on enhanced lte support for aerial vehicles," 2017.
- [4] A. Al-Hourani, S. Kandeepan, and A. Jamalipour, "Modeling air-to-ground path loss for low altitude platforms in urban environments," in *2014 IEEE Global Communications Conference*, 2014, pp. 2898–2904.
- [5] D. Kim, J. Lee, and T. Q. S. Quek, "Performance analysis for multi-layer unmanned aerial vehicle networks," in *2018 IEEE Globecom Workshops (GC Wkshps)*, 2018, pp. 1–6.
- [6] Q. Wu, W. Mei, and R. Zhang, "Safeguarding wireless network with uavs: A physical layer security perspective," *IEEE Wireless Communications*, vol. 26, no. 5, pp. 12–18, 2019.
- [7] A. Al-Hourani, S. Kandeepan, and S. Lardner, "Optimal lap altitude for maximum coverage," *IEEE Wireless Communications Letters*, vol. 3, no. 6, pp. 569–572, 2014.
- [8] W. Khawaja, I. Guvenc, D. W. Matolak, U.-C. Fiebig, and N. Schneckenburger, "A survey of air-to-ground propagation channel modeling for unmanned aerial vehicles," *IEEE Communications Surveys Tutorials*, vol. 21, no. 3, pp. 2361–2391, 2019.
- [9] J. Liu, M. Sheng, R. Lyu, and J. Li, "Performance analysis and optimization of uav integrated terrestrial cellular network," *IEEE Internet of Things Journal*, vol. 6, no. 2, pp. 1841–1855, 2019.
- [10] R. Amer, W. Saad, and N. Marchetti, "Toward a connected sky: Performance of beamforming with down-tilted antennas for ground and uav user co-existence," *IEEE Communications Letters*, vol. 23, no. 10, pp. 1840–1844, 2019.
- [11] G. Xin, W. Chen, and K. Liao, "Optimization of uav ultra-low altitude flight control system," in *2021 IEEE 4th Advanced Information Management, Communicates, Electronic and Automation Control Conference (IMCEC)*, vol. 4. IEEE, 2021, pp. 128–132.
- [12] H. Li, K. Feng, W. Cheng, and Y. Zhou, "Estimation of low-altitude wind-shear wind speed based on ddd-efa under aircraft yawing," in *2021 CIE International Conference on Radar (Radar)*. IEEE, 2021, pp. 3106–3111.
- [13] D. S. Lakew, A. Masood, and S. Cho, "3d uav placement and trajectory optimization in uav assisted wireless networks," in *2020 International Conference on Information Networking (ICOIN)*. IEEE, 2020, pp. 80–82.
- [14] P. Yu, Y. Ding, Z. Li, J. Tian, J. Zhang, Y. Liu, W. Li, and X. Qiu, "Energy-efficient coverage and capacity enhancement with intelligent uav-

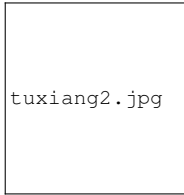
- bss deployment in 6g edge networks," *IEEE Transactions on Intelligent Transportation Systems*, 2022.
- [15] D. Pang, T. Shan, P. Ma, W. Li, S. Liu, and R. Tao, "A novel spatiotemporal saliency method for low-altitude slow small infrared target detection," *IEEE Geoscience and Remote Sensing Letters*, vol. 19, pp. 1–5, 2021.
- [16] S. Gong, M. Wang, B. Gu, W. Zhang, D. T. Hoang, and D. Niyato, "Bayesian optimization enhanced deep reinforcement learning for trajectory planning and network formation in multi-uav networks," *IEEE Transactions on Vehicular Technology*, 2023.
- [17] J. Liu, M. Sheng, R. Lyu, and J. Li, "Performance analysis and optimization of uav integrated terrestrial cellular network," *IEEE Internet of Things Journal*, vol. 6, no. 2, pp. 1841–1855, 2018.
- [18] E. Wang, W. Shu, J. Zhu, S. Xu, P. Qu, and T. Pang, "Low-altitude uav recognition and classification algorithm based on machine learning," in *2021 IEEE 16th Conference on Industrial Electronics and Applications (ICIEA)*. IEEE, 2021, pp. 1136–1141.
- [19] P. J. Singh and R. De Silva, "Design and implementation of an experimental uav network," in *2018 international conference on information and communications technology (icciact)*. IEEE, 2018, pp. 168–173.
- [20] Y. Chen, H. Zhang, and M. Xu, "The coverage problem in uav network: A survey," in *Fifth International Conference on Computing, Communications and Networking Technologies (ICCCNT)*. IEEE, 2014, pp. 1–5.
- [21] J. Lee and V. Friderikos, "Interference-aware path planning optimization for multiple uavs in beyond 5g networks," *Journal of Communications and Networks*, vol. 24, no. 2, pp. 125–138, 2022.
- [22] D. Kim, J. Lee, and T. Q. S. Quek, "Multi-layer unmanned aerial vehicle networks: Modeling and performance analysis," *IEEE Transactions on Wireless Communications*, vol. 19, no. 1, pp. 325–339, 2020.
- [23] Y. Du, H. Zhang, and J. Peng, "Modeling and coverage analysis for cellular-connected uavs with up-tilted antenna," *IEEE Communications Letters*, vol. 26, no. 11, pp. 2572–2575, 2022.
- [24] K. Yonezawa, T. Maeyama, H. Iwai, and H. Harada, "Path loss measurement in 5 ghz macro cellular systems and consideration of extending existing path loss prediction methods," in *2004 IEEE Wireless Communications and Networking Conference (IEEE Cat. No.04TH8733)*, vol. 1, 2004, pp. 279–283 Vol.1.
- [25] Q. Feng, J. McGeehan, E. Tameh, and A. Nix, "Path loss models for air-to-ground radio channels in urban environments," in *2006 IEEE 63rd Vehicular Technology Conference*, vol. 6, 2006, pp. 2901–2905.
- [26] B. Van Der Bergh, A. Chiumento, and S. Pollin, "Lte in the sky: trading off propagation benefits with interference costs for aerial nodes," *IEEE Communications Magazine*, vol. 54, no. 5, pp. 44–50, 2016.
- [27] Y. A. Novikova and M. B. Ryzhikov, "Research of requirements for the antenna pattern of the airborne weather radar to the reduce of false detection of hazards turbulence areas in low-altitude flight conditions," in *2020 Wave Electronics and its Application in Information and Telecommunication Systems (WECONF)*, 2020, pp. 1–7.
- [28] G. T. 36.873, "Study on 3d channel model for lte," 2018.
- [29] R. Bellman, *Combinatorial processes and dynamic programming*. Rand Corporation, 1958.
- [30] K. A. Dines and R. J. Lytle, "Computerized geophysical tomography," *Proceedings of the IEEE*, vol. 67, no. 7, pp. 1065–1073, 1979.
- [31] G. T. 38.901, "Study on channel model for frequencies from 0.5 to 100 ghz," 2023.
- [32] D. Grib, O. Sukharevsky, and G. Zalevsky, "Numerical modeling of ultrawideband signals scattered by low-altitude resonant targets," in *2016 8th International Conference on Ultrawideband and Ultrashort Impulse Signals (UWBUSIS)*. IEEE, 2016, pp. 93–96.
- [33] K. Yonezawa, T. Maeyama, H. Iwai, and H. Harada, "Path loss measurement in 5 ghz macro cellular systems and consideration of extending existing path loss prediction methods," in *2004 IEEE Wireless Communications and Networking Conference (IEEE Cat. No. 04TH8733)*, vol. 1. IEEE, 2004, pp. 279–283.
- [34] E. Artin, *The gamma function*. Courier Dover Publications, 2015.
- [35] I. S. Association *et al.*, "Ieee standard for broadband over power line networks: Medium access control and physical layer specifications," *IEEE std*, vol. 2010, no. 2010, pp. 1–1586, 1901.
- [36] T. Li, C. Li, C. Yang, J. Shao, Y. Zhang, L. Pang, L. Chang, L. Yang, and Z. Han, "A mean field game-theoretic cross-layer optimization for multi-hop swarm uav communications," *Journal of Communications and Networks*, vol. 24, no. 1, pp. 68–82, 2021.
- [37] A. Almarhabi, A. J. Aljohani, and M. Moinuddin, "Lora and high-altitude platforms: Path loss, link budget and optimum altitude," in *2020 8th International Conference on Intelligent and Advanced Systems (ICIAS)*. IEEE, 2021, pp. 1–6.



JIAO.ZHOU was born in HuNan, China in 1983. She received the B.S. and M.S. degrees in South China University of Technology, GuangZhou, in 2005. From 2014 to 2023, she was worked in China Mobile Communications Corporation Research Institute, senior researcher and engineer. She has been engaged in the planning and construction of 4/5G networks, as well as solutions to network problems. Participated in the development of multiple industry and enterprise standards.



XIN.LI Master's degree student, professor level senior engineer, engaged in technical research in the field of wireless communication.



LEI.CAO Doctoral, professor level senior engineer, consistently committed to current network technology innovation, international and domestic standard formulation, product research and development, and international cooperation in the fields of 4G, IoT, 5G wireless and terminal.